Multistatic Radar Workshop 2025
June, 19, 2025 – Milan, Italy

SURFACE TARGETS VELOCITY VECTOR ESTIMATION EXPLOITING CONSTELLATIONS OF SAR SYSTEMS

DEPARTMENT OF INFORMATION ENGINEERING,
ELECTRONICS AND TELECOMMUNICATIONS

SAPIENZA
UNIVERSITÀ DI ROMA

Ylenia D'Onofrio, Debora Pastina, Pierfrancesco Lombardo

RRSN Group
Radar Remote Sensing & Navigation

Introduction & Objective of the work

- Synthetic Aperture Radar (SAR): **all-weather** and **all-day image** capabilities
  - Largely used for continuous monitoring of **Surface moving target monitoring** (civil and military applications)

- In general velocity estimation techniques exploit effects induced by uncompensated target motion in the SAR image focused with respect to the stationary scene

R.Klemm; U.Nickel; C.Gierull; P.Lombardo; H.Griffiths; W.Koch. "Novel radar techniques andapplicationsVol.1",2017

Introduction & Objective of the work

- Synthetic Aperture Radar (SAR): **all-weather** and **all-day image** capabilities
  - Largely used for continuous monitoring of **Surface moving target monitoring** (civil and military applications)

- In general velocity estimation techniques exploit effects induced by uncompensated target motion in the SAR image focused with respect to the stationary scene

- **Along-track velocity** → Defocusing effect

R.Klemm; U.Nickel; C.Gierull; P.Lombardo; H.Griffiths; W.Koch. "Novel radar techniques andapplicationsVol.1",2017

Introduction & Objective of the work

- Synthetic Aperture Radar (SAR): **all-weather** and **all-day image** capabilities
  - Largely used for continuous monitoring of **Surface moving target monitoring** (civil and military applications)

- In general velocity estimation techniques exploit effects induced by uncompensated target motion in the SAR image focused with respect to the stationary scene

- **Along-track velocity** → Defocusing effect
- **Radial velocity** → Azimuth displacement

R.Klemm; U.Nickel; C.Gierull; P.Lombardo; H.Griffiths; W.Koch. "Novel radar techniques andapplicationsVol.1",2017

Objective of the work

- **Dual-channel single platform SAR**
  Availability of along-track interferometric phase:
  - Radial motion information
  - Traditionally used for ocean currents estimation
  - Joint exploitation with sub-aperture approaches or refocusing based approaches (i.e. residual doppler rate μ_{res})

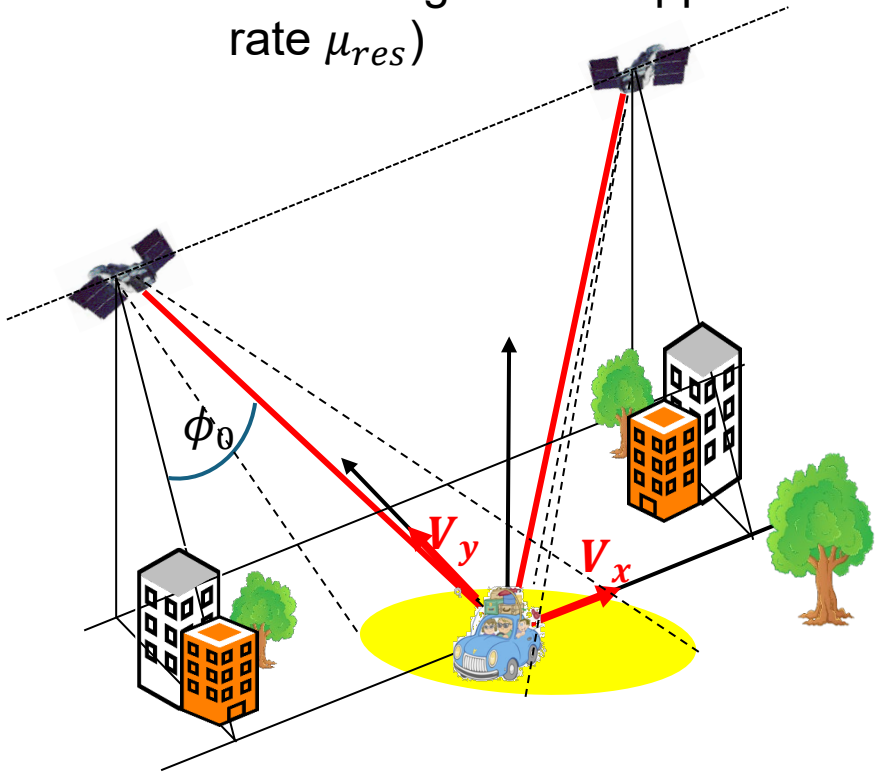

- **New Space Era → small satellite constellations** (ICEYE, Capella Space, Umbra…):
  - High resolution wide swath solutions
  - Few examples of motion estimation techniques

Focus of the work

- **Full velocity vector estimation method** of surface movers detected in SAR images acquired by **two SAR platforms,** each one with **dual antenna** receiver
- **joint** exploitation of two **along-track interferometric phase (ATI)**

Outline

- Interferometric SAR geometry and signal model
- Discussion of the estimation method
- Velocity vector estimation performance
- Theoretical analysis
- Optimization Strategy
- Conclusions

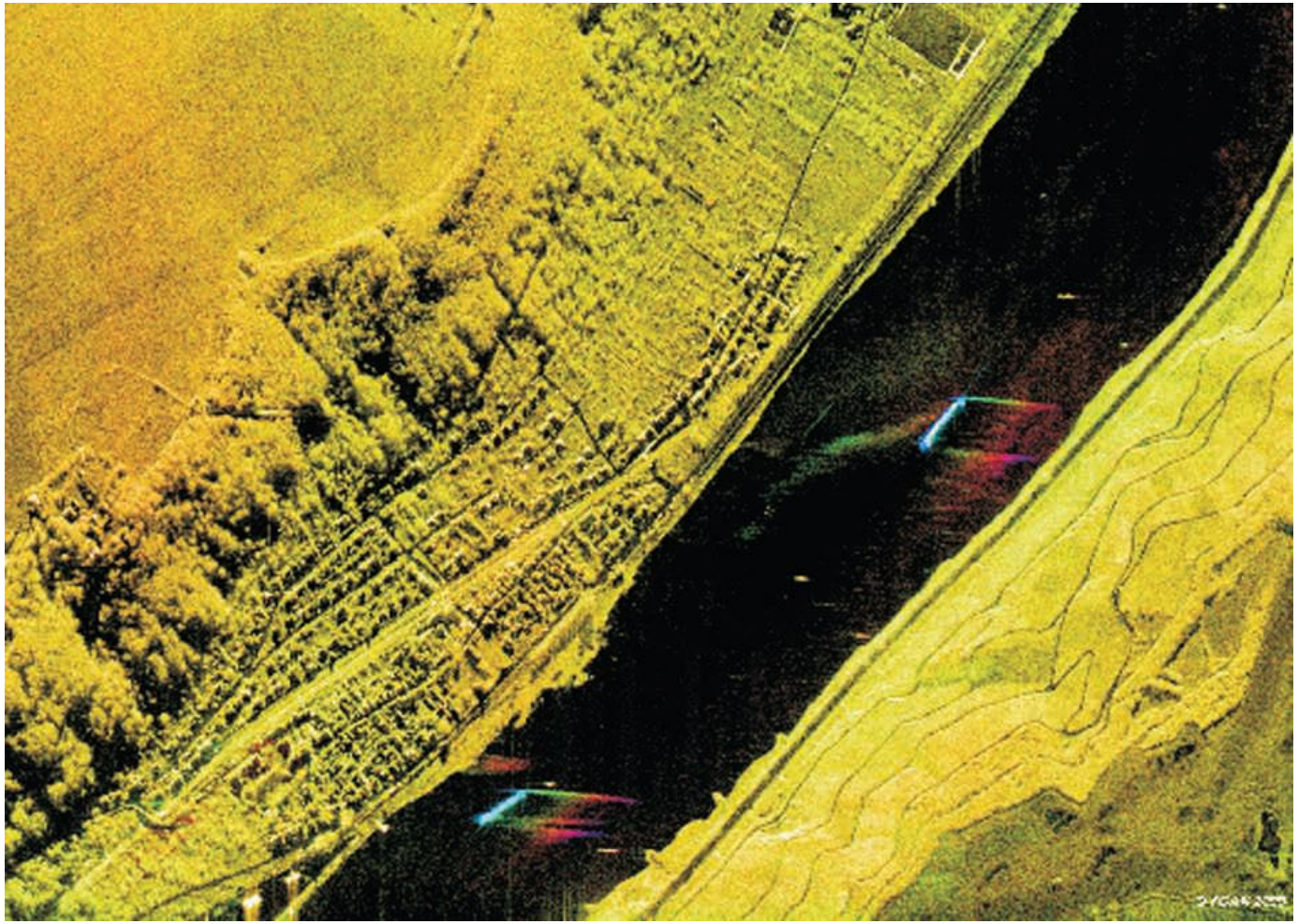

A. Budillon, C. H. Gierull, V. Pascazio and G. Schirinzi, "Along-Track Interferometric SAR Systems for Ground-Moving Target Indication: Achievements, Potentials, and Outlook," in IEEE Geoscience and Remote Sensing Magazine, vol. 8, no. 2, pp. 46-63, June 2020

Interferometric SAR geometry and signal model

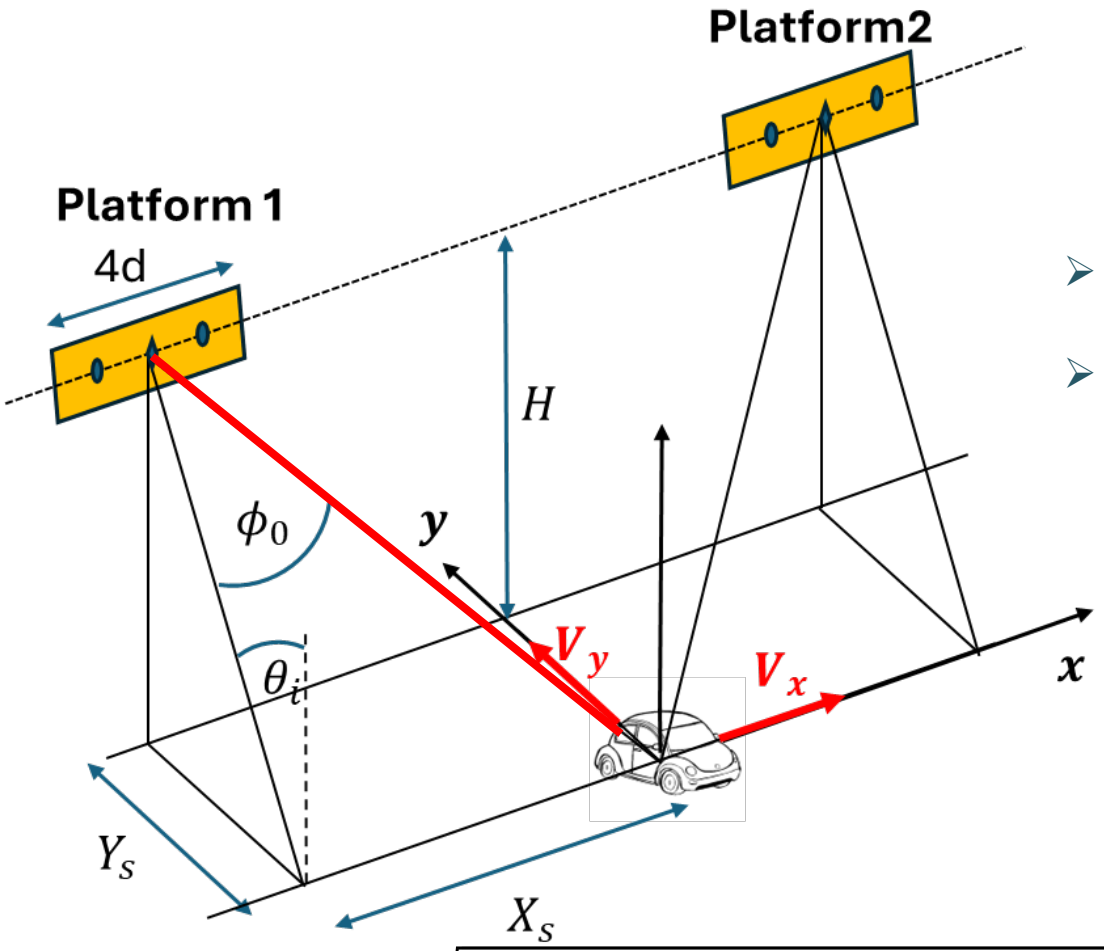

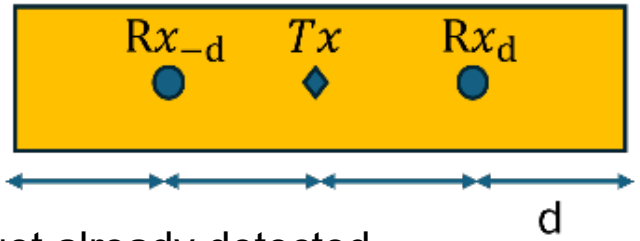

- Moving Target already detected
- **Range compressed signal** by the i-th receiving channel ($i = 0,1$) in slow time domain t, from k-platform

$$s_{ik}(t) = rect_{B_{Tk}-A_{Tk}}\left(t - \frac{B_{Tk}+A_{Tk}}{2}\right) e^{-\frac{j2\pi}{\lambda}\phi_k(X_{sk},Y_s,H,V_x,V_y,t)}$$

- B_{Tk}, A_{Tk}: Temporal extremes of Target visibility window
- Two-way bistatic range distance in the phase term:

$$\phi_k = \sqrt{H^2 + (X_{sk} + (V - V_x)t)^2 + \left(Y_s - V_y t\right)^2} + \sqrt{H^2 + (X_{sk} + d_i + (V - V_x)t)^2 + \left(Y_s - V_y t\right)^2}$$

Estimation Algorithm

$s_{0k}(t)$ $s_{1k}(t)$

Estimation Algorithm

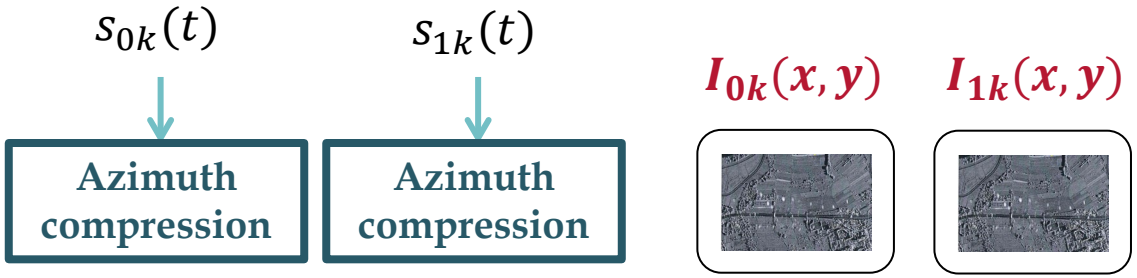

Estimation Algorithm

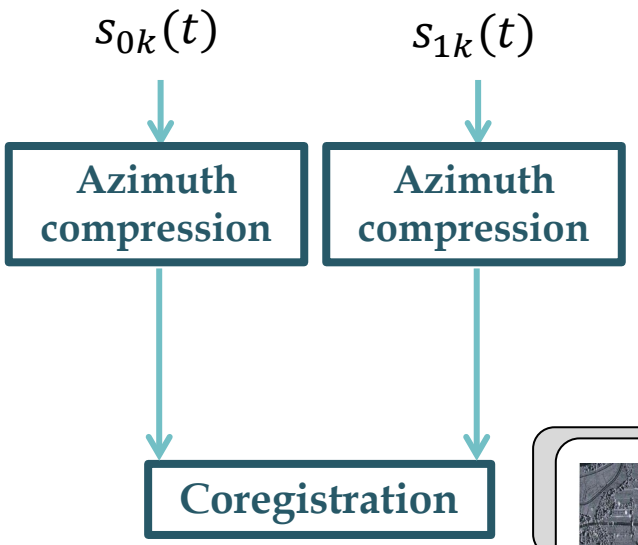

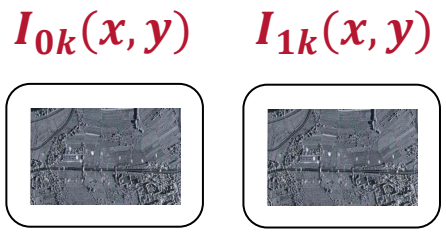

- **Linearized Model**

$$I_{ik}\left(x_{p_k}, y_{p_k}\right) \cong \int_{\max\left(A_{Tk}, A_{Fk}+\frac{x_{pk}}{V}\right)+\frac{d_i}{2V}}^{\min\left(B_{Tk}, B_{Fk}+\frac{x_{pk}}{V}\right)+\frac{d_i}{2V}} e^{j\frac{4\pi}{\lambda}(R_{Fk}-R_{Tik})+j\frac{4\pi}{\lambda}\mathrm{N}_{ik}\left(t-\frac{x_{pk}}{V}\right)+j\pi\mu_{res,ik}\left(t-\frac{x_{pk}}{V}\right)^2} dt$$

Estimation Algorithm

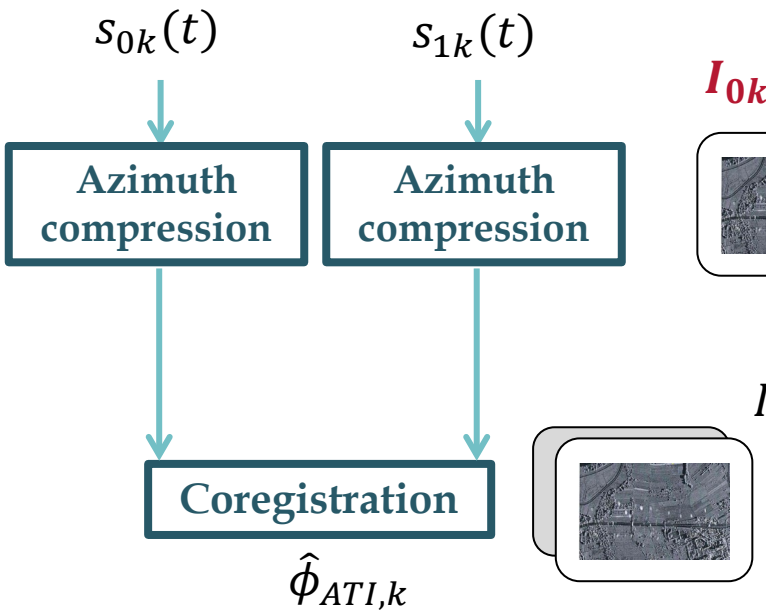

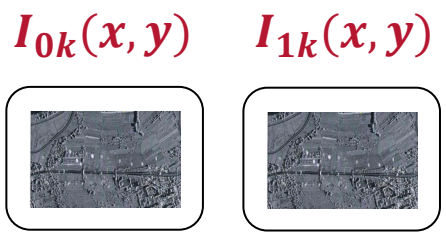

➢ Linearized Model

$$I_{ik}\left(x_{p_k}, y_{p_k}\right) \cong \int_{\max\left(A_{Tk}, A_{Fk}+\frac{x_{pk}}{V}\right)+\frac{d_i}{2V}}^{\min\left(B_{Tk}, B_{Fk}+\frac{x_{pk}}{V}\right)+\frac{d_i}{2V}} e^{j\frac{4\pi}{\lambda}\left(R_{Fk}-R_{Tik}\right)+j\frac{4\pi}{\lambda}\mathrm{N}_{ik}\left(t-\frac{x_{pk}}{V}\right)+j\pi\mu_{res,ik}\left(t-\frac{x_{pk}}{V}\right)^2} dt$$

➢ Measurements Model

$$\phi_{ATI,k} \simeq \angle I_{0k} I_{1k}^* \cong \frac{4\pi}{\lambda}\left(R_{T1k}-R_{T0k}\right) \cong \frac{4\pi}{\lambda V} d\left(\frac{-\left(X_{sk}+\frac{(V-V_x)x_{pk}}{V}\right)V}{R_{F_K}}+V_{radial}\right)$$

$$V_{radial} = \frac{-V_y\left(Y_s - V_y\frac{x_{pk}}{V}\right)+(V-V_x)(X_{sk}+(V-V_x)\frac{x_{pk}}{V})}{R_{Fk}}$$

Estimation Algorithm

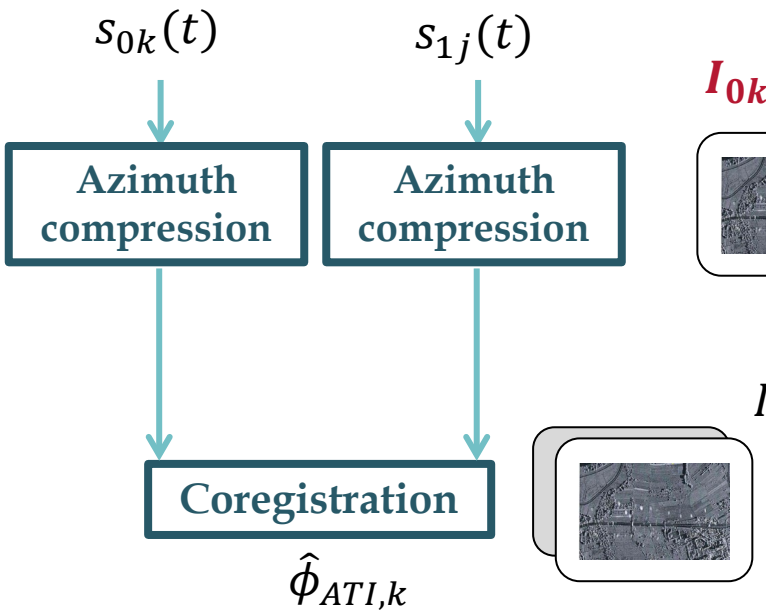

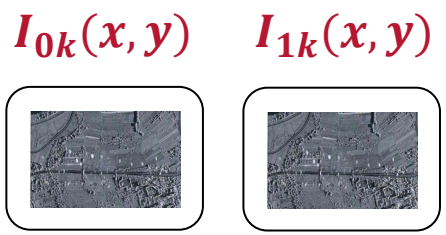

Linearized Model

$$I_{ik}(x_{p_k}, y_{p_k}) \cong \int_{\max\left(A_{Tk}, A_{Fk}+\frac{x_{pk}}{V}\right)+\frac{d_i}{2V}}^{\min\left(B_{Tk}, B_{Fk}+\frac{x_{pk}}{V}\right)+\frac{d_i}{2V}} e^{j\frac{4\pi}{\lambda}(R_{Fk}-R_{Tik})+j\frac{4\pi}{\lambda}\mathrm{N}_{ik}\left(t-\frac{x_{pk}}{V}\right)+j\pi\mu_{res,ik}\left(t-\frac{x_{pk}}{V}\right)^2} dt$$

Measurements Model

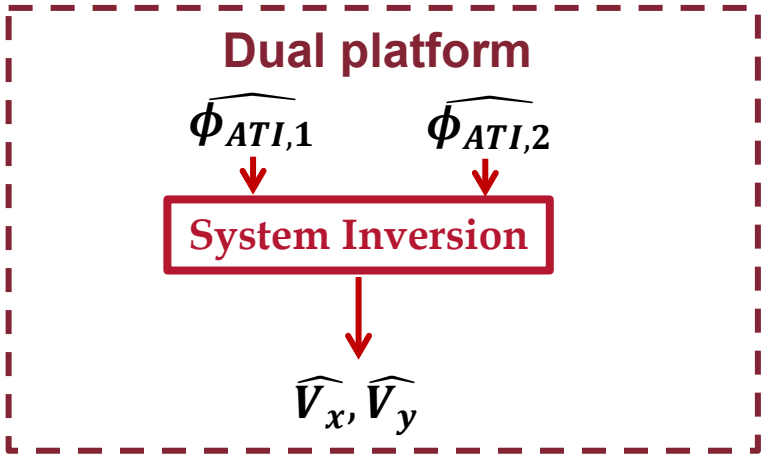

$$\phi_{ATI,k} \simeq \angle I_{0k} I_{1k}^* \cong \frac{4\pi}{\lambda}(R_{T1k} - R_{T0k}) \cong \frac{4\pi}{\lambda V} d \left(\frac{-\left(X_{sk} + \frac{(V-V_x)x_{pk}}{V}\right)V}{R_{F_K}} + V_{radial} \right)$$

$$V_{radial} = \frac{-V_y\left(Y_s - V_y\frac{x_{pk}}{V}\right) + (V-V_x)(X_{sk} + (V-V_x)\frac{x_{pk}}{V})}{R_{Fk}}$$

Performance analysis

- Complex SAR image amplitude corrupted by **zero mean additive white gaussian disturbance**

- **Small error approximation** for estimation accuracies $\sigma_{\delta V_x}$ and $\sigma_{\delta V_y}$
  → measurements errors $\delta\phi_{ATI1}, \delta\phi_{ATI2}$ mapped in target velocity estimation errors $\delta V_x, \delta V_y$:

$$\begin{bmatrix} \sigma^2_{\delta V_x} & 0 \\ 0 & \sigma^2_{\delta V_y} \end{bmatrix} = Z^{-1} \begin{bmatrix} \sigma^2_{\phi_{ATI1}} & 0 \\ 0 & \sigma^2_{\phi_{ATI2}} \end{bmatrix} \mathrm{Z}^{-1^{\mathrm{T}}} \qquad Z = \begin{bmatrix} \frac{\partial \phi_{ATI1}}{\partial(\delta V_x)} & \frac{\partial \phi_{ATI1}}{\partial(\delta V_y)} \\ \frac{\partial \phi_{ATI2}}{\partial(\delta V_x)} & \frac{\partial \phi_{ATI2}}{\partial(\delta V_y)} \end{bmatrix}$$

- **Measurements variances**

$$\sigma^2_{\phi k} * = \int_{-\pi}^{\pi} \frac{\left(\phi' - \phi_{Meanj}\right)^2 \left(1 - |\rho_{ck}|^2\right)}{2\pi \left(1 - \left(|\rho_{ck}| \cos\left(\phi' - \phi_{ATI,k}\right)\right)^2\right)} \left(1 + \frac{|\rho_{ck}| \cos\left(\phi' - \phi_{ATI,k}\right) \arccos\left(-|\rho_{ck}| \cos\left(\phi' - \phi_{ATI,k}\right)\right)}{\sqrt{1 - \left(|\rho_{ck}| \cos\left(\phi' - \phi_{ATI,k}\right)\right)^2}}\right) d\phi'$$

$$\rho_{ck} = \frac{1}{1 + \frac{1}{SNR_k}}$$

* Li , Q. He, "On the Ratio of Two Correlated Complex Gaussian Random Variables," in *IEEE CL*, vol.23, no. 12, pp. 2172-2176, Dec. 2019

Performance analysis

- Complex SAR image amplitude corrupted by **zero mean additive white gaussian disturbance**

- **Small error approximation** for estimation accuracies $\sigma_{\delta V_x}$ and $\sigma_{\delta V_y}$
  → measurements errors $\delta\phi_{ATI1}, \delta\phi_{ATI2}$ mapped in target velocity estimation errors $\delta V_x, \delta V_y$:

$$\begin{bmatrix} \sigma^2_{\delta V_x} & 0 \\ 0 & \sigma^2_{\delta V_y} \end{bmatrix} = Z^{-1} \begin{bmatrix} \sigma^2_{\phi_{ATI1}} & 0 \\ 0 & \sigma^2_{\phi_{ATI2}} \end{bmatrix} Z^{-1^{\mathrm{T}}} \qquad Z = \begin{bmatrix} \frac{\partial \phi_{ATI1}}{\partial(\delta V_x)} & \frac{\partial \phi_{ATI1}}{\partial(\delta V_y)} \\ \frac{\partial \phi_{ATI2}}{\partial(\delta V_x)} & \frac{\partial \phi_{ATI2}}{\partial(\delta V_y)} \end{bmatrix}$$

- **Measurements variances**

$$\sigma^2_{\phi k} * = \int_{-\pi}^{\pi} \frac{(\phi' - \phi_{Meanj})^2 (1 - |\rho_{ck}|^2)}{2\pi \left(1 - (|\rho_{ck}| \cos(\phi' - \phi_{ATI,k}))^2\right)} \left(1 + \frac{|\rho_{ck}| \cos(\phi' - \phi_{ATI,k}) \arccos(-|\rho_{ck}| \cos(\phi' - \phi_{ATI,k}))}{\sqrt{1 - (|\rho_{ck}| \cos(\phi' - \phi_{ATI,k}))^2}}\right) d\phi'$$

$$\rho_{ck} = \frac{1}{1 + \frac{1}{\overline{SNR_k}}}$$

Signal-to-Noise Ratio

* Li , Q. He, "On the Ratio of Two Correlated Complex Gaussian Random Variables," in *IEEE CL*, vol.23, no. 12, pp. 2172-2176, Dec. 2019

Case study

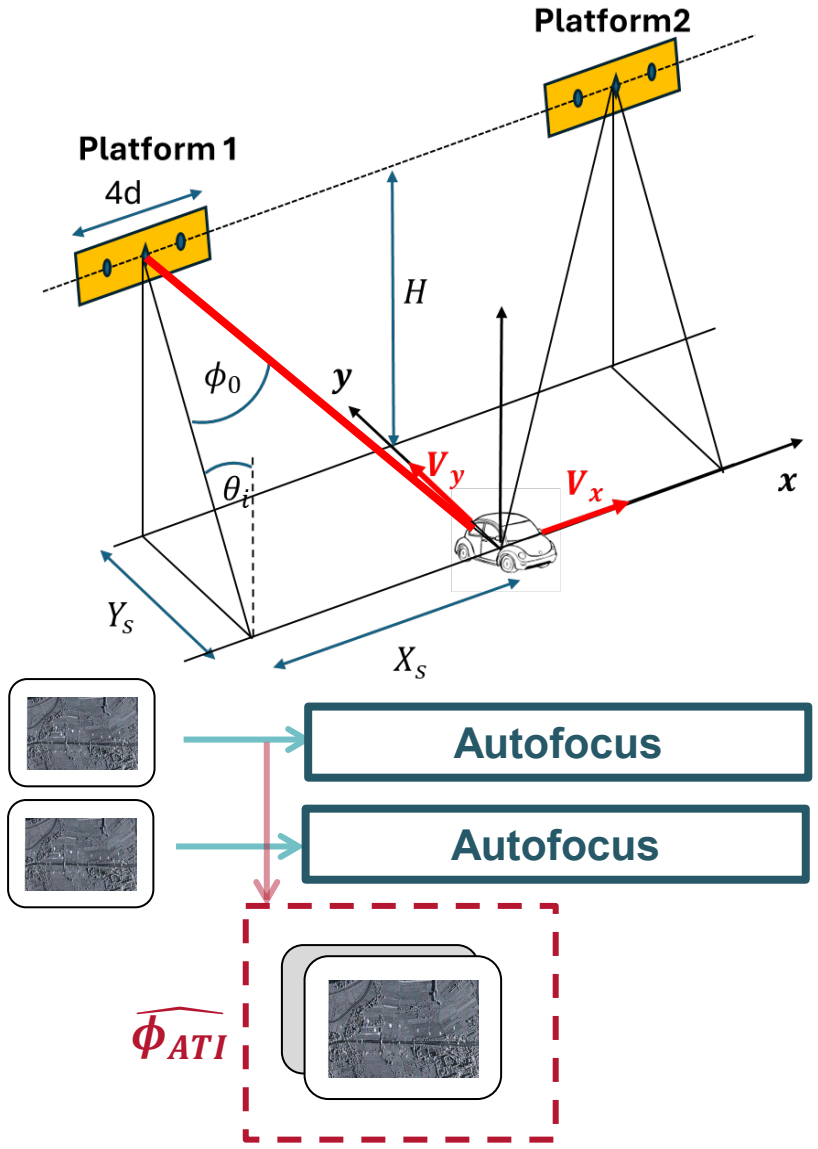

➢ Common LEO satellite parameters

H	570000 m	d	6/4 m
Y_s	265795,36 m	λ	0,03 m
θ_i	25°	V	7,5 km/s

➢ Squint Angle

- High squint geometry $\phi_0 = 26°$

➢ Signal-to-Noise Ratio (SNR)

- Interferometric phase before autofocus $SNR = SNR(V_x, V_y)$,

➢ Moving Target motion

Slant range velocity ($V_y sin\theta_i$) and along-track velocity (V_x) ranging from -20 m/s to 20 m/s

Case study

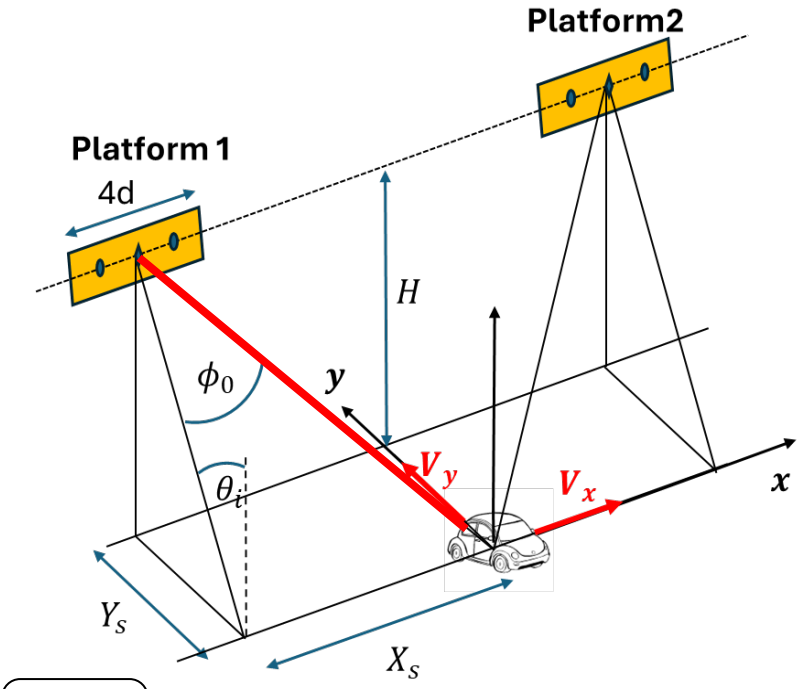

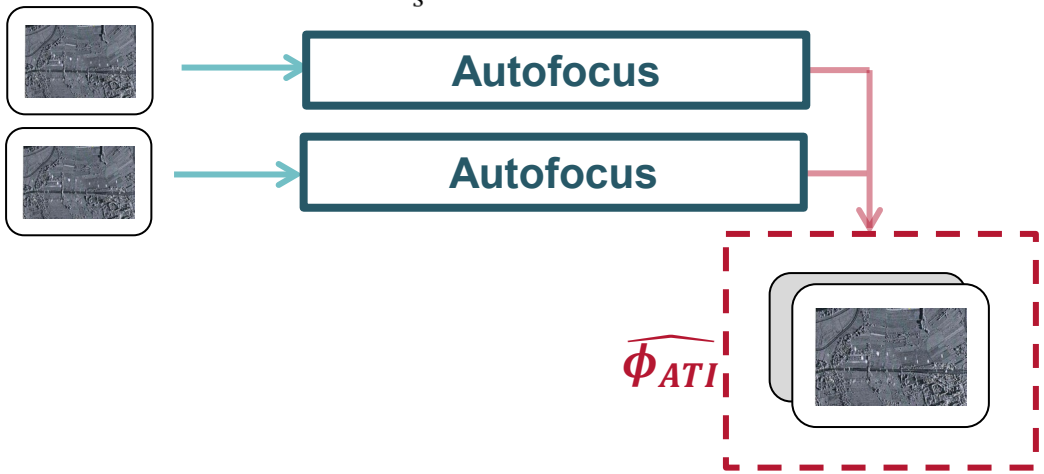

➢ Common LEO satellite parameters

H	570000 m	d	6/4 m
Y_s	265795,36 m	λ	0,03 m
θ_i	25°	V	7,5 km/s

➢ Squint Angle

- High squint geometry $\phi_0 = 26°$

➢ Signal-to-Noise Ratio (SNR)

- Interferometric phase before autofocus $SNR = SNR(V_x, V_y)$,
- Interferometric phase after autofocus $SNR = SNR_0$

$$SNR_0 = SNR(0,0) = [100,1000]\, cos\phi_0^4$$

➢ Moving Target motion

Slant range velocity ($V_y sin\theta_i$) and along-track velocity (V_x) ranging from -20 m/s to 20 m/s

Performance assessment results

❑ Interferometric phase before autofocus

$$SNR_k = SNR_k(V_x, V_y) = SNR_0 \frac{|I_{ik}(x_{pk}, y_{pk})|^2}{(B_{Fk} - A_{Fk})^2}$$

➢ The estimation error is affected by the SNR worsening due to **defocusing effect**

Standard Deviation of $\widehat{V_x}$

$SNR_0 = 100\cos\phi_0^4$

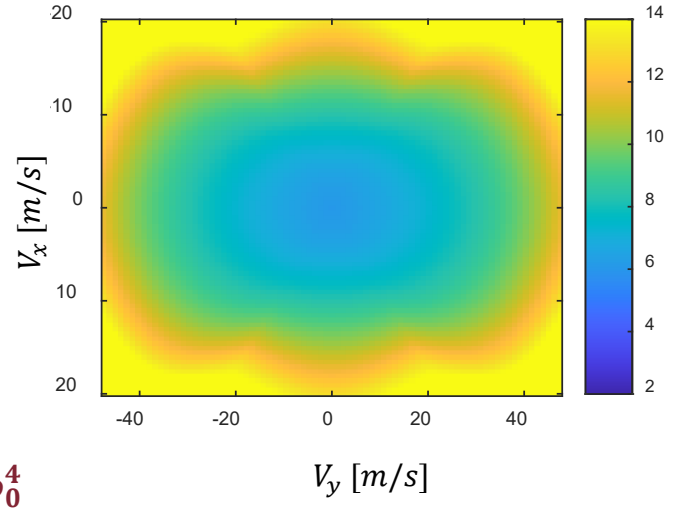

$SNR_0 = 1000\cos\phi_0^4$

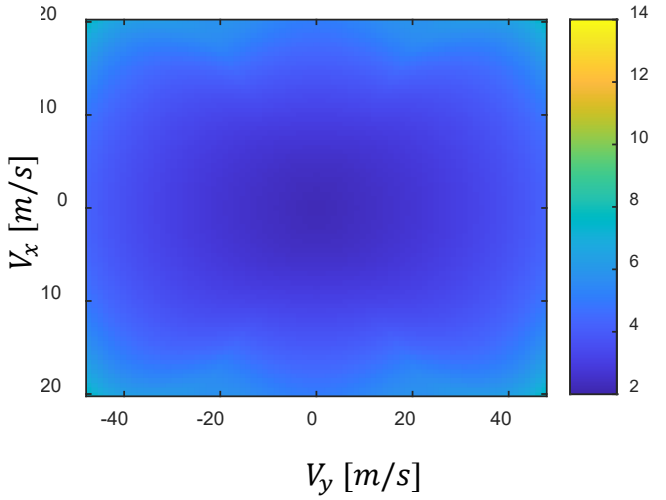

Standard Deviation of $\widehat{V_y}$

$SNR_0 = 100\cos\phi_0^4$

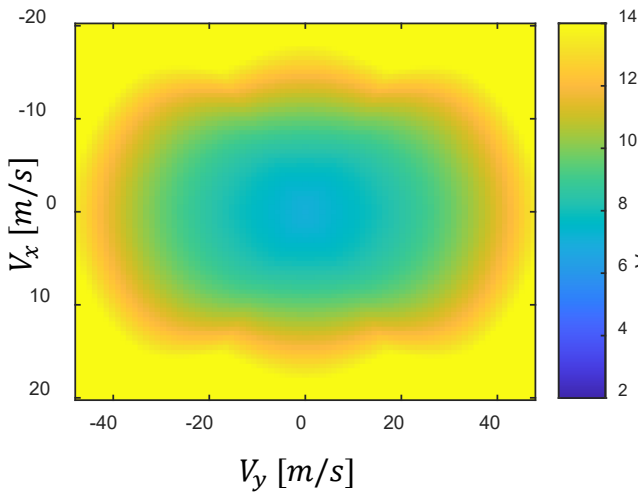

$SNR_0 = 1000\cos\phi_0^4$

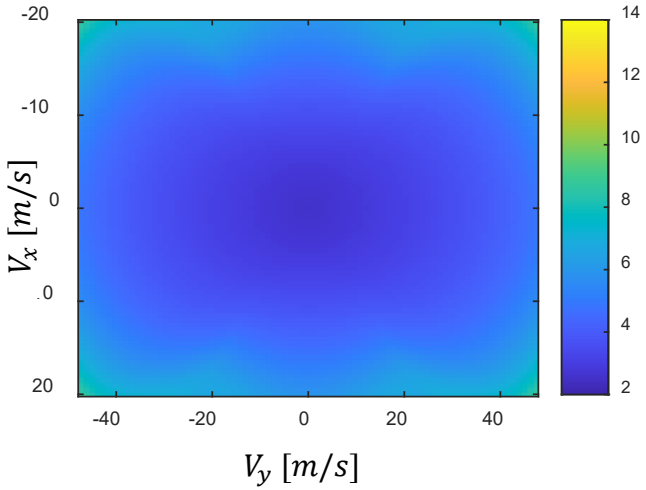

➢ As the **SNR increases**, a general **improvement** in performance can be observed

➢ **Theoretical analysis validation** theoretical results and Monte Carlo simulations largely in agreement

Performance assessment results

❑ Interferometric phase after Autofocus

$$SNR = SNR_0 = 1000cos^4\phi_0$$

- Maximum SNR for all motion conditions
  - general **improvement** at high velocities;
  - Estimation variances independent of velocity→ searching for optimum configuration

Standard Deviation of $\widehat{V_x}$

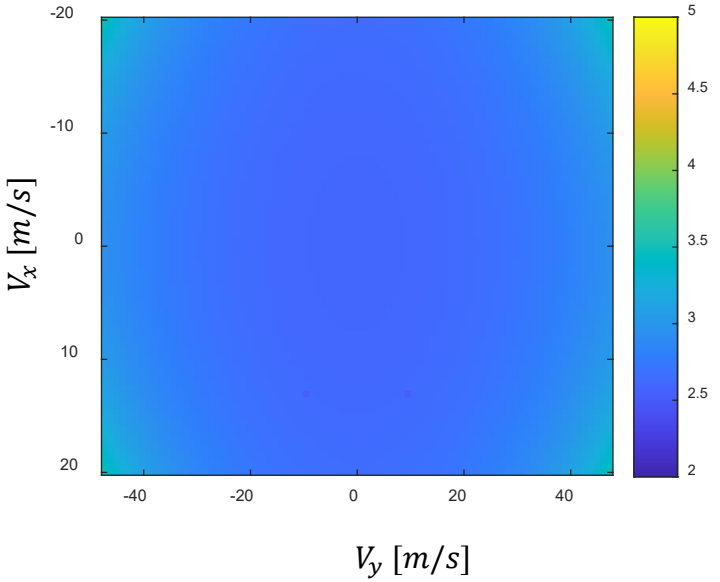

Standard Deviation of $\widehat{V_y}$

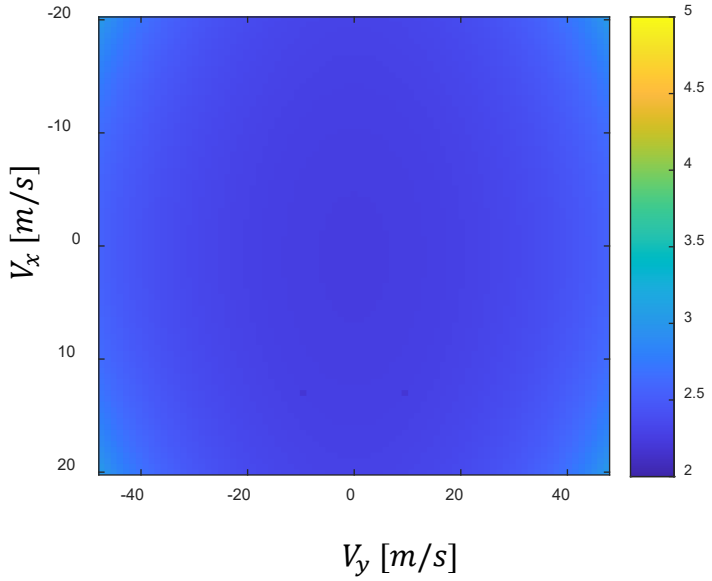

- Best performance: Standard Deviation of V_x and $V_y \geq 2$ m/s

- **Theoretical analysis validation**
  theoretical results and Monte Carlo simulations largely in agreement

Optimization of the two-satellite constellation

- Increasing Squint angle

  - Smaller SNR due to range attenuation
  - Higher sensitivity to along-track velocity
  - Worse cross-track estimation capability

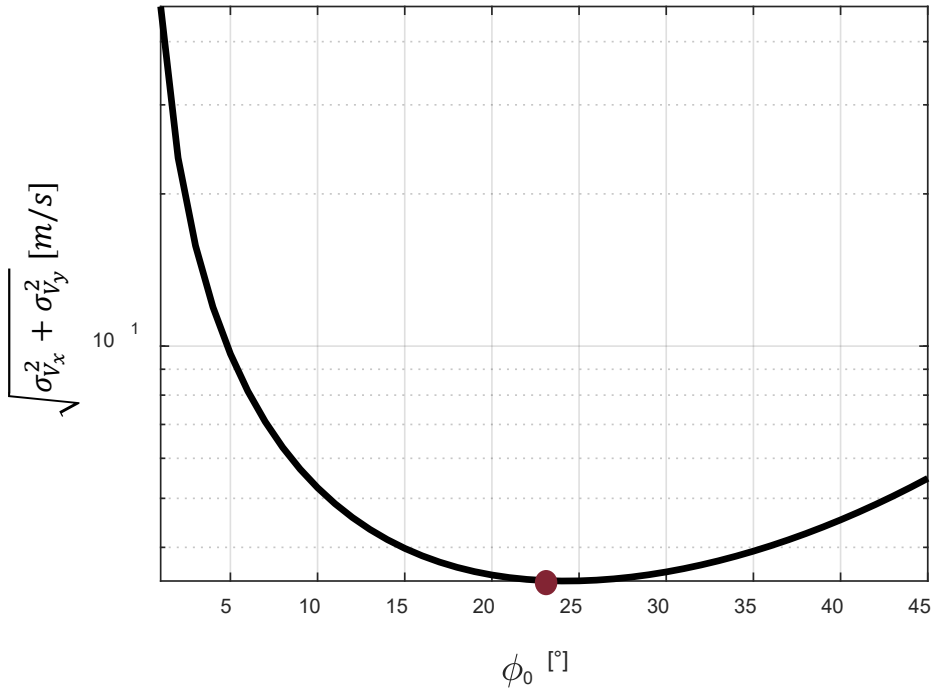

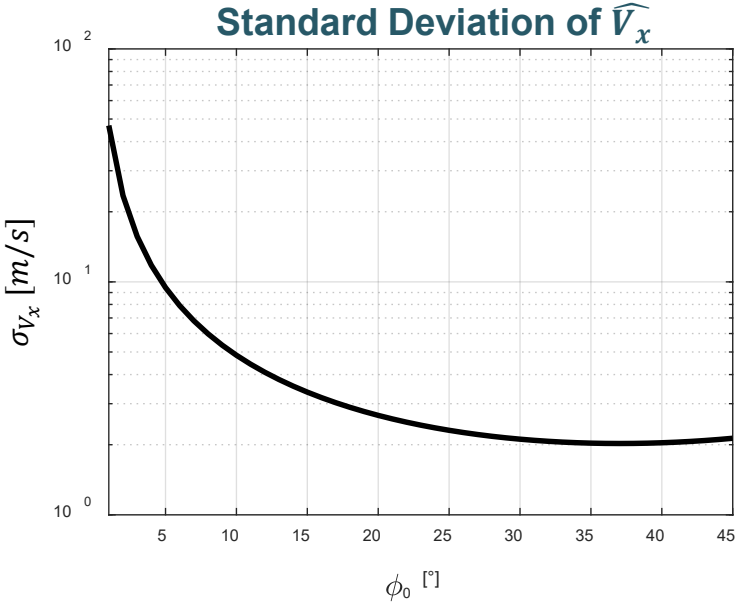

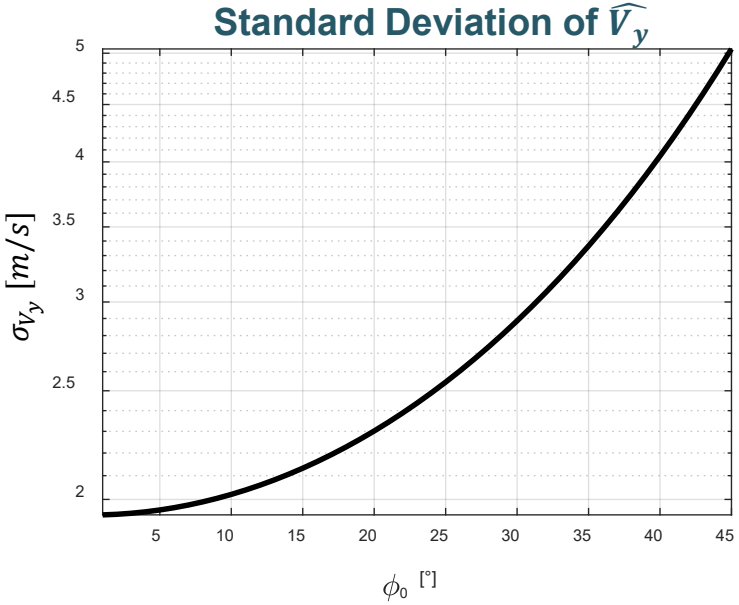

Optimization Strategy

$$\mathrm{F}(V_x, V_y) = \min\left(\sqrt{\sigma_{V_x}^2 + \sigma_{V_y}^2}\right) \rightarrow$$

Optimal Squint Angle

24°

Conclusions

- **Velocity vector estimation technique and validation** using a Dual-channel Dual-platform SAR system

- **Performance analysis has shown that**:
  - Considerable improvement in estimation accuracy is obtained through refocusing
  - Optimal configuration with squint angle $\phi_0 = 24°$ provides $\sigma_{V_x}, \sigma_{V_y} \cong 2\ m/s$

- **On going & Future Work**

- Refocusing provides residual Doppler rate measurement μ_{res}: joint exploitation of multiple SAR observables

  - **Multi-channel solutions** (for example: Single-platform dual-channel* case study: μ_{res} and ϕ_{ATI}) or **Multi-static multi-channel solutions** (for example: Dual-platform dual-channel case study: μ_{res} and ϕ_{ATI})
  - **Multi-static single-channel solutions** (for example: Dual-platform single-channel case study: μ_{res} only)
  - **MIMO solutions**
  - **Multi-channel techniques distributed on multiple single-channel platforms**

- Generalization to cope with more complex target motion models (e.g. accelerating targets)
- Investigating the impact of **variations in platform geometry** on the achievable performance

*Y. D'Onofrio, D. Pastina, P. Lombardo, "Target Velocity Vector Estimation from Single Platform Dual-Channel Squinted Synthetic Aperture Radar", 2025 International Radar Symposium, Hamburg (Germany).